Research Article

The concentration effects on structural and magnetic properties of $Fe_2V_{1-x}Mn_xGe$ Heusler alloys

C. Boyraz[1] · A. Guler[2] · P. Aksu[3] · L. Arda[4]

Received: 6 January 2022 / Accepted: 20 June 2022
Published online: 27 June 2022

Abstract
This study presents the concentration-dependent structural, morphological, and magnetic properties of $Fe_2V_{1-x}Mn_xGe$ Heusler alloys (x = 0.0, 0.25, and 0.50) have not been studied previously in the literature, and are investigated by using X-ray Diffractometer, Scanning Electron Microscope (SEM), and Physical Properties Measurement System (PPMS). We observed from the X-ray diffraction measurements that (except x = 0) $Fe_2V_{1-x}Mn_xGe$ samples have had $L2_1$-type crystal structure, matching well with the literature. In all SEM images, some holes and crack-type formations are observed. Increasing Mn content in $Fe_2V_{1-x}Mn_xGe$ Heusler alloys can effectively inhibit grain boundary migration. Except for Fe_2VGe, the other alloys in the series are investigated to be soft ferromagnets at 5 K with saturation magnetic moment. The (M-H) graphs especially for $Fe_2V_{0.75}Mn_{0.25}Ge$ and $Fe_2V_{0.5}Mn_{0.5}Ge$ measured at 5 K reveal almost no coercive fields and easy magnetization. Namely, the system easily saturates without needing any high fields. The obtained results show that these new samples may be suitable candidates for technological applications.

Article highlights

- The arc-melting method is used to synthesize new $Fe_2V_{1-x}Mn_xGe$ cubic Heusler alloys.
- Both increment of Mn and decrement V in the structure, reveal phase transition from hexagonal DO_{19} to cubic $L2_1$ form.
- The M-H graphs for $Fe_2V_{1-x}Mn_xGe$ alloys measured at 5 K present almost no coercive fields and easy magnetization.

Keywords Heusler alloys · Sintering procedure · Structural and magnetic properties

1 Introduction

Heusler alloys that exhibit half-metal behavior have an important place in industrial applications in terms of versatile physical properties and spintronic applications. These compounds, which also had triple intermetallic properties, were found by Fritz Heusler in 1903 [1, 2]. Heusler alloys with the face-centered cubic structure are found in the forms of XYZ (half Heusler), X_2YZ (full Heusler), inverse-Heusler (Y_2XZ), and quaternary-Heusler (XX'YZ). Most of these types of compounds have become quite a subject of study with their characteristics such as topological insulator, magnetoresistance, semiconductor, superconductivity, ferromagnetism, ferrimagnetism, and antiferromagnetic which are related to

✉ C. Boyraz, cboyraz@marmara.edu.tr | [1]Faculty of Technology, Department of Mechanical Engineering, Marmara University, Maltepe, 34840 Istanbul, Turkey. [2]Faculty of Technology, Department of Electrical and Electronics Engineering, Marmara University, Maltepe, 34840 Istanbul, Turkey. [3]Institute of Nanotechnology, Gebze Technical University, Gebze, 41400 Kocaeli, Turkey. [4]Faculty of Engineering and Naturel Sciences, Department of Mechatronic Engineering, Bahcesehir University, Besiktas, 34349 Istanbul, Turkey.

spintronics. Some new developments on half-metallic materials which have fully spin-polarized are still on the attention of researchers [3]. With the property of zero total magnetic moments, half-metallic antiferromagnets are also the focus of the research due to low energy loss. An important feature of most Heusler alloys is that the physical category entered by the alloy can be determined by counting the valence electrons [4, 5]. Another important feature of Heusler alloys is that the energy band ranges can be adjusted between 0 and ~ 4 eV by changing the chemical composition. Due to this feature, Heusler alloys are among the important candidates for both solar cell and thermoelectric applications [6–9].

The optimization of the crystal structure by using varying atoms with different radii or annealing temperatures and durations is essential for the creation of the desired physical and chemical properties. Previous studies are mostly on substituting V in one of the Fe sites in Fe_3Ge under the condition of higher annealing temperature [10]. To our best knowledge, there are a few studies on $Fe_{3-x}V_xGe$ but neither experimentally nor theoretically, there is not yet a detailed report on the Mn-doped $Fe_2V_{1-x}Ge$ compound. In cubic Heusler alloys, the inherently low magneto-crystalline anisotropy can be a limiting factor in spintronic and magnetic applications [4]. A hexagonal Heusler analogue retaining half metallicity and exhibiting a high magnetocrystalline anisotropy should be very interesting for spin-torque-transfer RAM (STT-RAM) [11]. In the literature, for half-metallicity, some hexagonal DO_{19} Heusler alloys (with the space group of P63/mmc) have been predicted [12–14]. In this study, for the first time, the properties of the structure, morphology, and magnetic properties of $Fe_2V_{1-x}Mn_xGe$ Heusler alloys obtained by the arc-melting method are detailed. The syntheses and physical properties of cubic $Fe_2V_{1-x}Mn_xGe$ Heusler alloys are detailed. The results are evaluated by the provided data. In the materials and methods section, the synthesizing conditions of the Heusler alloys and the details of measurement techniques are summarized. An overview of the conducted research is provided using some important details in the conclusion section experimental results and their correlations with each other and literature are provided in the results and discussion section.

2 Materials and methods

The 99,999% pure Fe, V, Mn, and Ge chemicals obtained from Sigma-Aldrich were synthesized by the arc-melting method by mixing them in appropriate proportions for final $Fe_2V_{1-x}Mn_xGe$ alloys. To obtain a homogeneous structure, the melting process was applied 5 times in the argon gas environment. The obtained samples were subjected to the heating and cooling treatment by applying a specific heating and cooling procedure. The samples were heated to 900 °C at a rate of 2 °C / min and kept at that temperature for 5 days. The samples were ground in an agate mortar to obtain the powder form for physical measurements. Then, the samples were released for the cooling process without a programmed decrease in the furnace. For the determination of the structural phases of the samples, a Bruker D8 Discover XRD device was used. Co Kα source with 40 kV voltage, 30 mA current, and λ = 1.79 Å wavelength were used in the measurements. The surfaces of the samples were sanded, smoothed, and polished to take the surface images using the Philips XL30 brand Scanning Electron Microscope (SEM). The elemental compositions of the formed structures were studied by the energy distribution spectrometer (EDS) unit connected to the SEM device. The magnetic measurements were provided under the maximum of 2 Tesla magnetic fields by the Quantum Design Physical Properties Measurement System (PPMS). Temperature-dependent magnetic field measurement data were obtained in the temperature range of 5–400 K by PPMS tool.

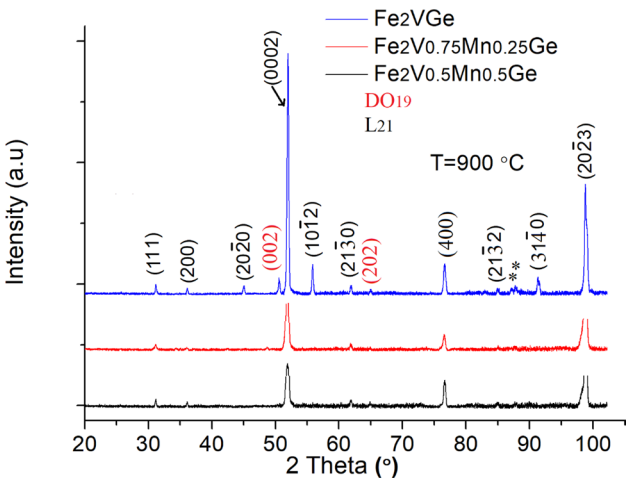

Fig. 1 The XRD patterns of $Fe_2V_{1-x}Mn_xGe$ compounds. Note that the indexes shown in red color belong to the possible DO_{19} hexagonal phase and the indexes in black color belong to $L2_1$ cubic phase [10, 13]

3 Results and discussions

The diffraction patterns of the $Fe_2V_{1-x}Mn_xGe$ samples prepared by the arc-melting method using Fe, V, Mn, and Ge elements were exhibited in Fig. 1. The arc melting process was repeated 5 times to obtain homogeneous structures. $Fe_{3-x}V_xGe$ composition which presents similar structural properties to $Fe_2V_{1-x}Mn_xGe$ possesses two space groups:

$L2_1$ Xa ($F\bar{4}3m$) and ($Fm\bar{3}m$) [10]. As seen in Fig. 1 given by blue color for Fe_2VGe, the structure is almost showing a sign of a good fit with the proposed crystal model $L2_1$. However, some additional peaks are given by the red color belonging to the DO_{19} crystal model [13]. It is known in the literature that possible site assignments for cubic. Adding Mn to the $Fe_2V_{1-x}Mn_xGe$ structure ($Fe_2V_{0.5}Mn_{0.5}Ge$ and $Fe_2V_{0.75}Mn_{0.25}Ge$) shows the disappearing small amount of DO_{19} ($P6_3/mmc$ no.194) peaks. This may indicate a reduction in structural defect and transition of the structure to a fully cubic state. The * symbol in Fig. 1 indicates the unknown peaks. The lattice parameters were calculated by X'Pert HighScore Plus software using XRD pattern and the results were checked by Cohen's method for $L2_1$ (space group 225) structure.

Both in terms of increasing Mn or decreasing V elements in the $Fe_2V_{1-x}Mn_xGe$ samples revealed a decrease in the value of in-plane lattice parameters and cell volume in Fig. 2a and b. As seen in Table 1, the effect of the V atom on the lattices and cell volume is quite small in the structure.

Using randomly selected regions of the samples, the surface morphology and elemental compositions of $Fe_2V_{1-x}Mn_xGe$ Heusler alloys were depicted in Fig. 3, 4, and 5 for the samples Fe_2VGe, $Fe_2V_{0.5}Mn_{0.5}Ge$, and $Fe_2V_{0.75}Mn_{0.25}Ge$ respectively. In all SEM images, some holes and crack-type formations were observed. This should be the reason for sanding, smoothing, polishing, and heat treatment before taking the SEM images [10, 15]. The colored SEM pictures also showed that the elements belong the compositions still existed after the heat treatment procedure. The SEM surface images have also awakened the idea of smooth, stuck well, and dense structures of all samples. This idea was also supported by EDX measurements in all micrographs of $Fe_2V_{1-x}Mn_xGe$ Heusler alloys by obtaining all necessary peaks of elements given in Figs. 3, 4, and 5c. The obtained stoichiometry for all chemical compositions was depicted in the inset tables of Figs. 3, 4, and 5c.

To reveal the average grain size, the SEM images in 100 µm frames were exhibited in Fig. 6. Increasing Mn content in $Fe_2V_{1-x}Mn_xGe$ Heusler alloys can effectively inhibit grain boundary migration. The magnetic moment variations due to the external magnetic field of the $Fe_2V_{1-x}Mn_xGe$ Heusler alloys obtained by the arc-melting process are exhibited in Fig. 7 at constant temperatures of 400 K, 300 K, and 5 K. The saturation magnetization values of all three different Fe_2VGe, $Fe_2V_{0.75}Mn_{0.25}Ge$, and $Fe_2V_{0.5}Mn_{0.5}Ge$ samples are 0.515 μ_B/f.u., 1.93 μ_B/f.u., and 1.781 μ_B/f.u. at 5 K measurements respectively. The highest magnetization was obtained for the $Fe_2V_{0.75}Mn_{0.25}Ge$ sample to be 1.93 μ_B/f.u. and doping enough Mn to the Fe_2VGe structure stabilized the system by saturating the

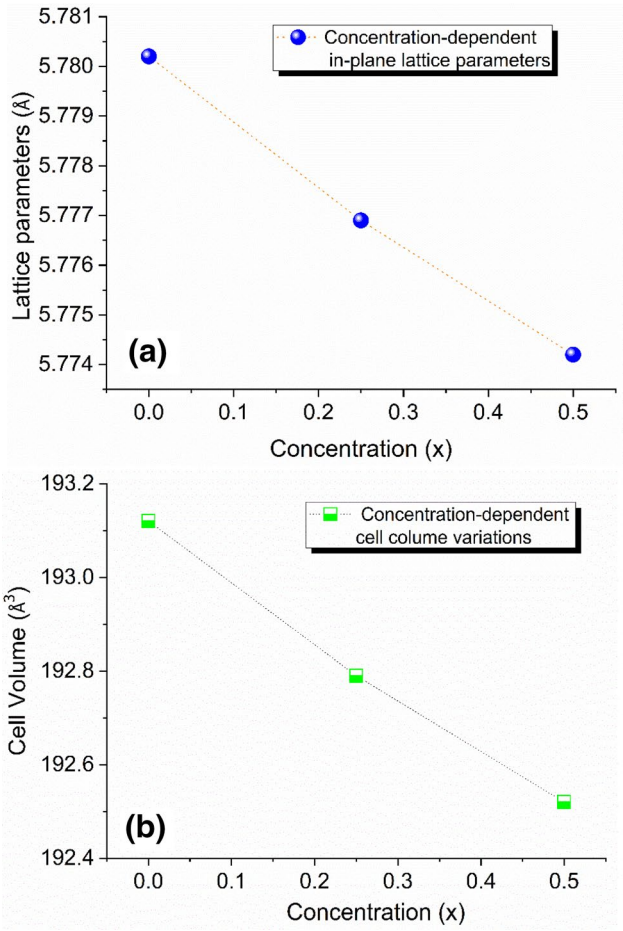

Fig. 2 In (**a**), the variation of concentration-dependent in-plane lattice parameters and concentration-dependent cell volume variation in (**b**)

Table 1 The variation of concentration-dependent, lattice parameters, and the unit cell volume

Sample formula	Experimental lattice a (Å)	Theoretical lattice a (Å)	Cell volume (Å^3)
Fe_2VGe	5.7674	5.7802	193.121
$Fe_2V_{0.75}Mn_{0.25}Ge$	5.7663	5.7769	192.790
$Fe_2V_{0.5}Mn_{0.5}Ge$	5.7649	5.7742	192.520

magnetic moments as seen in Fig. 7b and c at 5 K. As seen in Fig. 7a–c, the magnetization (M-H) curves due to the magnetic field taken at a temperature of 5 K creates a negligible coercive field, while at the 300 K and 400 K (M-H) curves, there is no coercive field and the ferromagnetic properties of the samples are lost at these temperatures [10]. In all $Fe_2V_{1-x}Mn_xGe$ Heusler systems, the annealing temperature is the predominant factor determining the characteristic behaviors of the investigated system. All $Fe_2V_{1-x}Mn_xGe$ Heusler alloys measured at 5 K exhibited

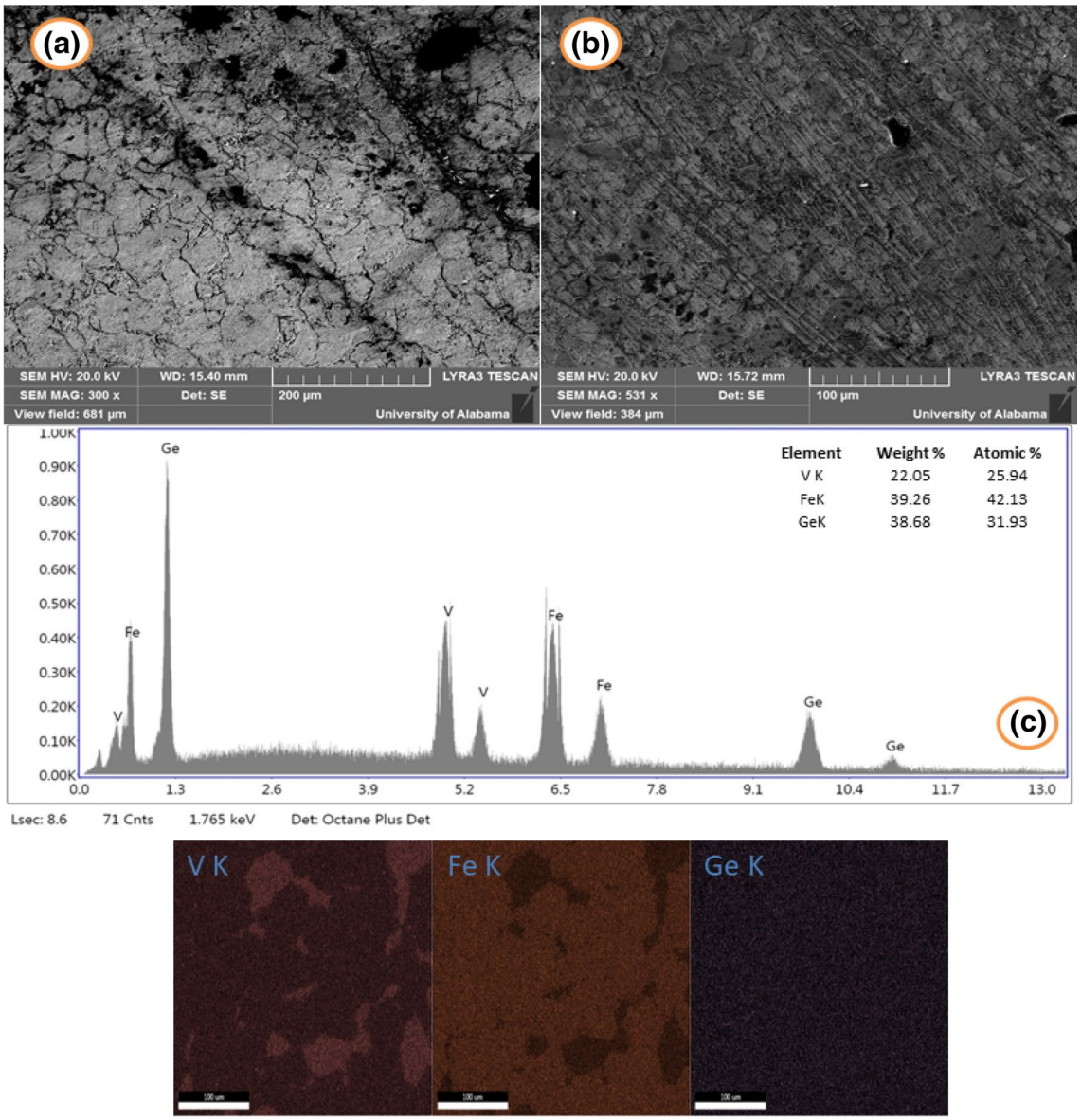

Fig. 3 SEM images in 200 and 100 µm frames in (**a**) and (**b**) and EDX micrograph with the atomic ratio in (**c**) and colored SEM images of V, Fe, and K elements for Fe_2VGe composition

ferromagnetic behavior and turned to paramagnetic when applied to higher temperatures (300 K and 400 K). The (M-H) graphs especially for $Fe_2V_{0.75}Mn_{0.25}Ge$ and $Fe_2V_{0.5}Mn_{0.5}Ge$ measured at 5 K in Fig. 7b and c reveals almost no coercive fields and easily magnetization [10]. Namely, the system easily saturates without needing any high fields. Therefore this result should be a significant indication of new material candidates for electric circuits working at low temperatures.

In Fig. 8, the temperature-dependent moment variations of $Fe_2V_{1-x}Mn_xGe$ Heusler alloys obtained by arc melting under the 2 Tesla magnetic field were observed. Zero field cooling (ZFC) and field cooling FC curves match well and depict a general decrease in the moment values with increasing temperature. This behavior is particularly consistent with the Curie law after T = 200 K.

Temperature-dependent magnetic moment variation was clarified by using $Fe_2V_{0.5}Mn_{0.5}Ge$ data and fitting it to the Curie–Weiss equation (red color). The fitting parameters were demonstrated in Fig. 9 and using the Table Curve program (linear and non-linear Curve fitting software package) $\mu_{eff} = 4.8$/ion was found.

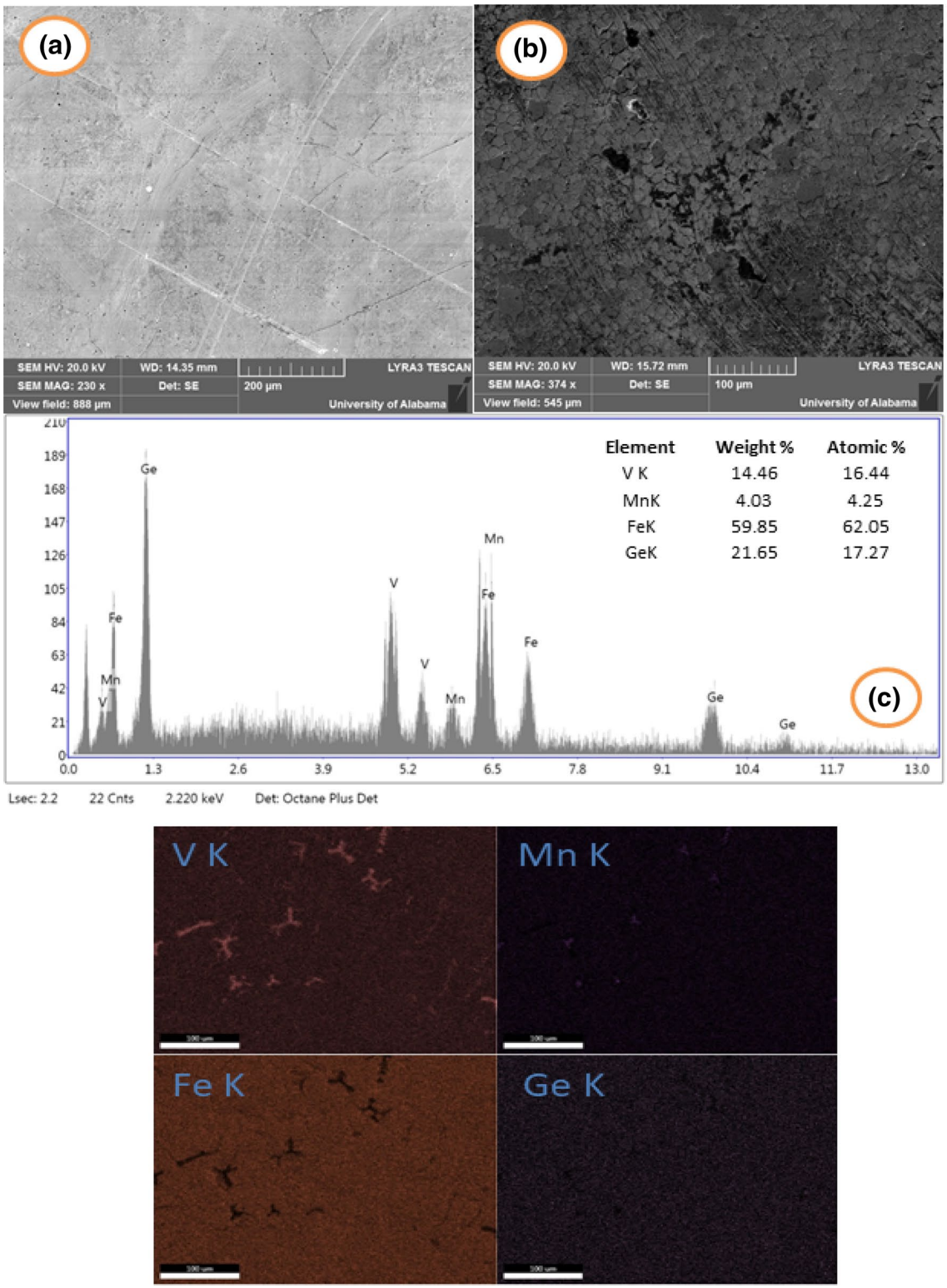

Fig. 4 SEM images in 200 and 100 µm frames in (**a**) and (**b**) and EDX micrograph with an atomic ratio in (**c**) and colored SEM images of V, Mn, Fe, and K elements for $Fe_2V_{0.75}Mn_{0.25}Ge$ composition

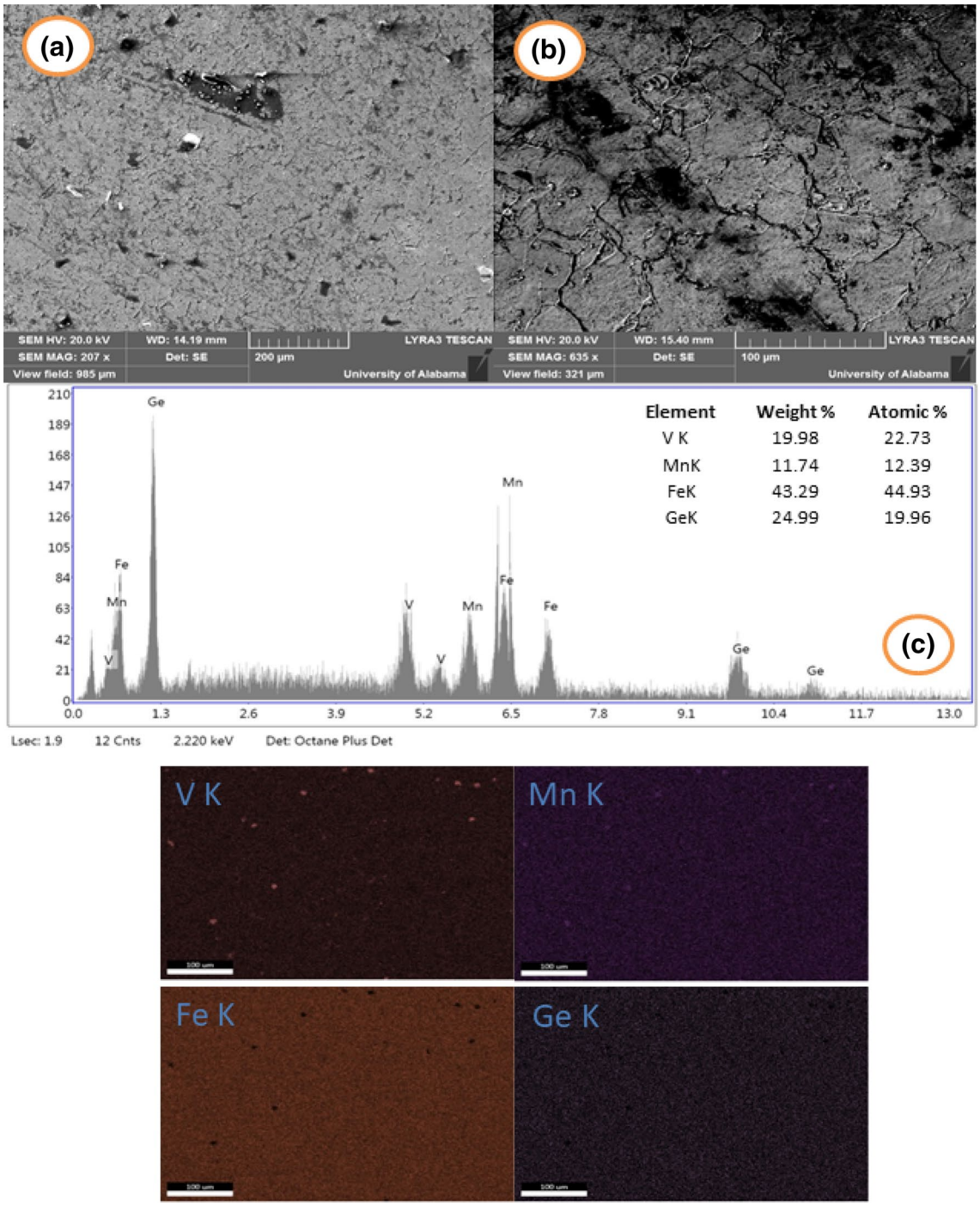

Fig. 5 SEM images in 200 and 100 µm frames in (**a**) and (**b**) and EDX micrograph with the atomic ratio in (**c**) and colored SEM images of V, Mn, Fe, and K elements for $Fe_2V_{0.5}Mn_{0.5}Ge$ composition

4 Conclusion

The $Fe_2V_{0.5}Mn_{0.5}Ge$ cubic structure was obtained using the arc melting method. Although a few minor DO_{19} peaks were observed in the Fe_2VGe sample, the main structure $L2_1$ was observed in $Fe_2V_{0.75}Mn_{0.25}Ge$ and $Fe_2V_{0.5}Mn_{0.5}Ge$ samples by doping Mn element. Thus, we conclude that DO_{19} hexagonal peaks in the structure were no longer visible by coexisting V and Mn elements in the structure. As observed in Fig. 6, increasing Mn

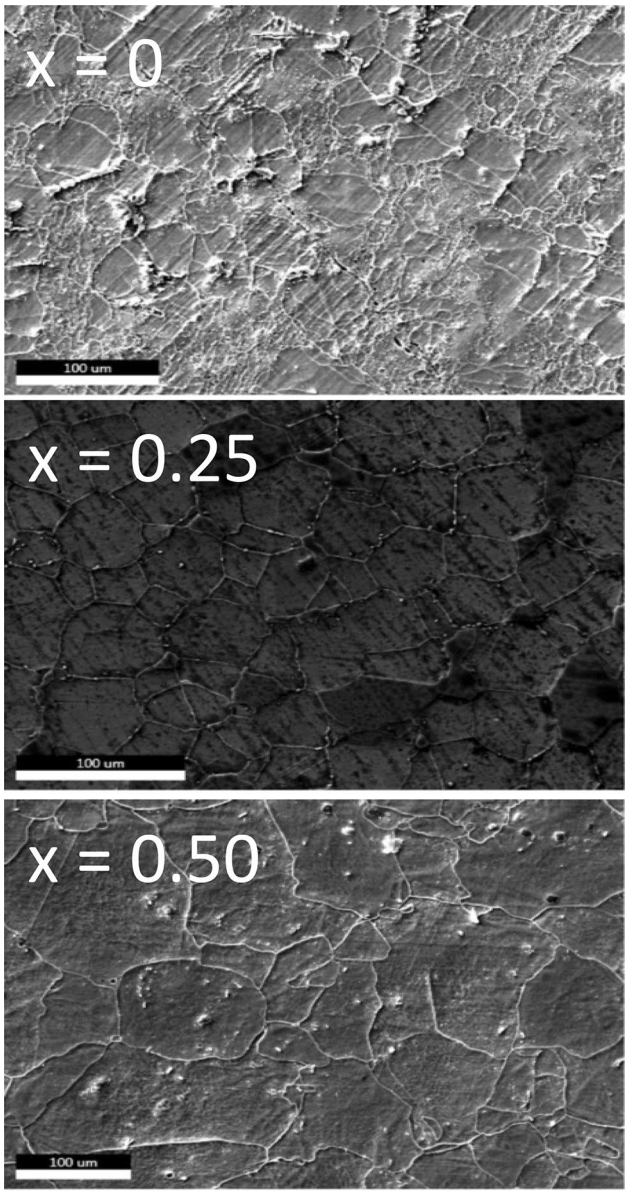

Fig. 6 SEM images in 100 µm frames for x = 0, x = 0.25, and x = 0.5 of $Fe_2V_{1-x}Mn_xGe$ Heusler alloys

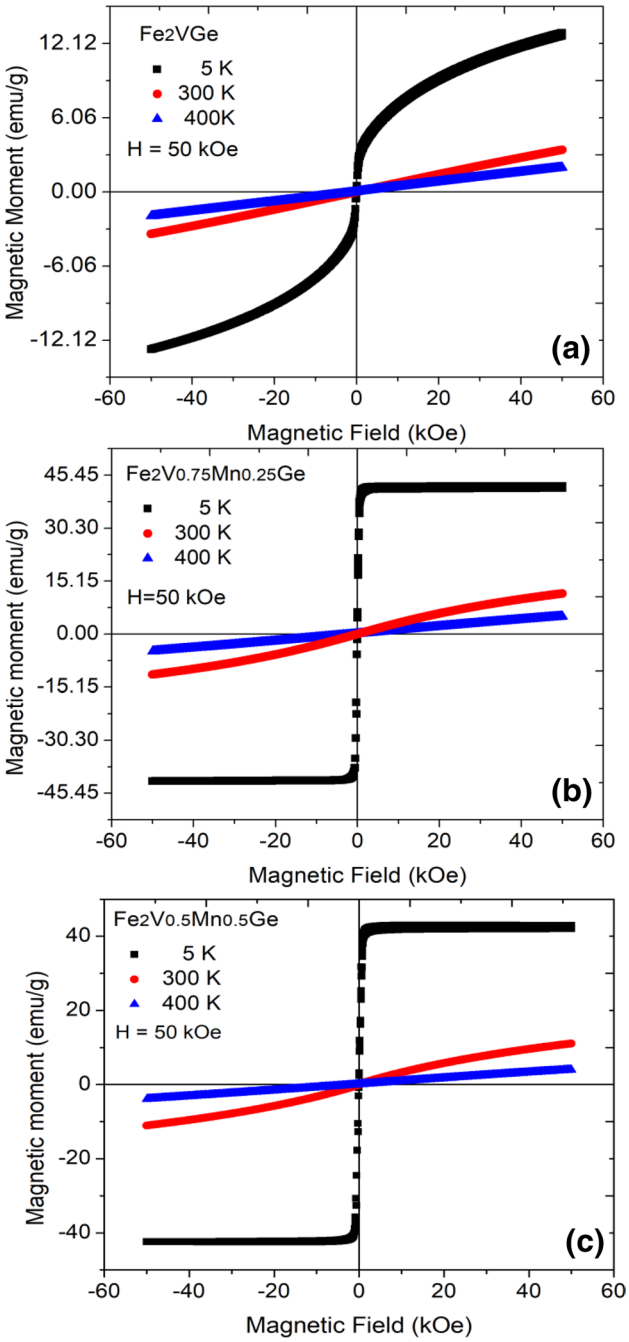

Fig. 7 (M-H) graphs of $Fe_2V_{1-x}Mn_xGe$ Heusler alloys under up to 50 kOe magnetic field and at 5 K, 300 K, and 400 K temperatures

content in $Fe_2V_{1-x}Mn_xGe$ Heusler alloys can effectively inhibit grain boundary migration. Except for Fe_2VGe, the other alloys in the series (x = 0.25 and x = 0.50) revealed soft ferromagnetic properties at 5 K with saturation magnetic moment. The (M-H) graphs especially for $Fe_2V_{0.75}Mn_{0.25}Ge$ and $Fe_2V_{0.5}Mn_{0.5}Ge$ measured at 5 K in Fig. 7b and c reveals almost no coercive fields and easily magnetization. Namely, the system easily saturates without needing any high fields. The obtained results show that these new samples may be suitable candidates for technological applications.

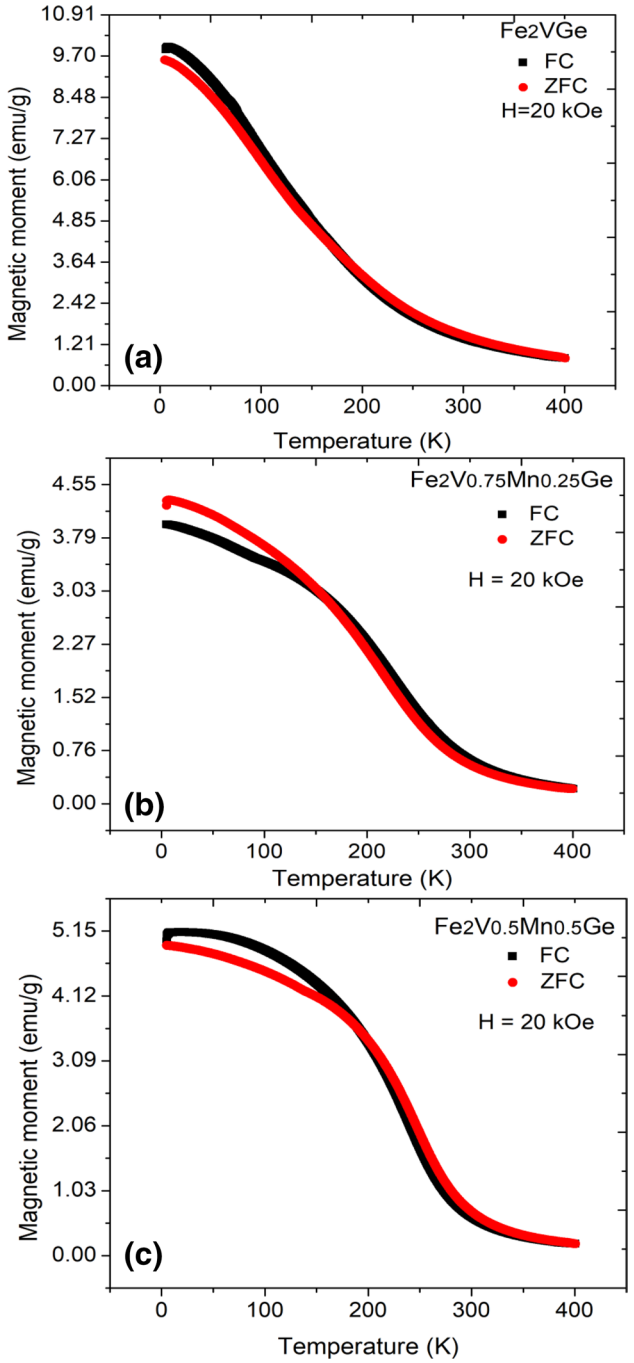

Fig. 8 (M-T) graphs of $Fe_2V_{1-x}Mn_xGe$ Heusler alloys measured at a wide temperature file up to room temperature

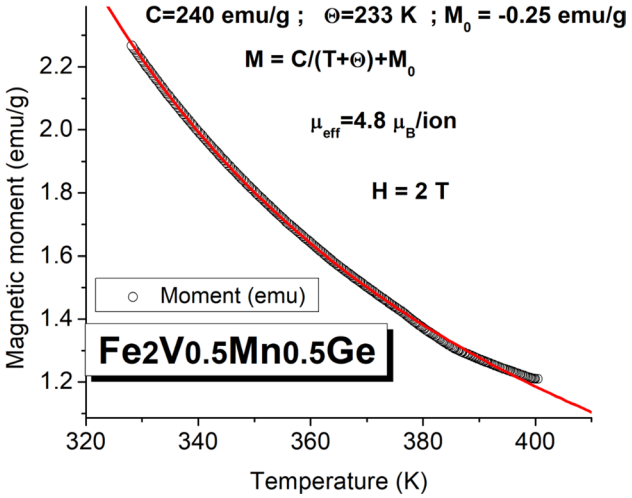

Fig. 9 The fitting of $Fe_2V_{0.5}Mn_{0.5}Ge$ to reveal T_c critical temperature and other parameters

Acknowledgements We convey our thanks to The University of Alabama for its laboratory facilities. We also thank Mrs. Serhat Guler for her financial support for this research.

Author Contributions CB Conceptualization, Methodology, Formal analysis and investigation, Validation, Writing-Reviewing and Editing, Writing- Original draft preparation, Writing- Reviewing and Editing. PA Methodology, Conceptualization, Methodology, Formal analysis and investigation, Validation, Writing- Original draft preparation. AG Conceptualization, Methodology, Formal analysis and investigation, Validation, Writing- Original draft preparation. LA Conceptualization, Methodology, Formal analysis and investigation, Validation, Writing-Reviewing and Editing, Writing- Original draft preparation, Validation, Writing- Reviewing and Editing, Supervision, and Funding acquisition.

Funding The presented work was supported by the Research Fund of Bahcesehir University (Project No: BAP-2021.01.27 and BAP.2019–01.04), and Research Fund of Marmara University (Project No: FYL-2022–10334), Istanbul, Turkey.

Data availability All data generated or analyzed during this study are included in this published article.

Declarations

Conflict of interest On behalf of all authors, the corresponding author states that there is no conflict of interest. The authors declare that they have no known competing financial interests or personal relationships that could have appeared to influence the work reported in this paper.

Ethical approval This article does not contain any studies with human participants or animals performed by any of the authors.

References

1. Graf T, Felser C, Parkin S (2011) Simple rules for the understanding of Heusler compounds. Prog Solid State Chem 39:1–50
2. Heusler F, Starck W, Haupt E (1903) Über magnetische Manganlegierungen. DPG 5:220–223
3. Wang XL (2008) Proposal for a new class of materials: spin gapless semiconductors. Phys Rev Lett 100:156404
4. Felser C, Fecher GH, Balke B (2007) Spintronics: a challenge for materials science and solid-state chemistry. Angew Chem Int Ed 46(5):668–699
5. Kübler J, William AR, Sommers CB (1983) Formation and coupling of magnetic moments in Heusler alloys. Phys Rev B 28:1745
6. Kratochvílov MD, Kral M, Du J, Valenta R, Colman O, Heczko M (2020) Fe_2MnSn-experimental quest for predicted heusler alloy. J Magn Magn Mater 501:166426
7. Xin F, You C, Fu H, Ma L, Cheng Z, Tian N (2020) Mechanically tuning magnetism and transport property in spin gapless semiconductor CoFeMnSi flexible thin film. J Alloys Compd 813:152207
8. Kainuma R, Imano Y, Ito W, Morito H, Okamoto S, Kitakami O (2006) Magnetic-field-induced shape recovery by reverse phase transformation. Nature 439:957–960
9. Chadov S, Qi X, Kübler J, Fecher GH, Felser C, Zhang SC (2010) Tunable multifunctional topological insulators in ternary Heusler compounds. Nat Mat 9:541–545
10. Mahat R, Shambhu KC, Wines D, Ersan F, Regmi S, Karki U, AtacaPadhan WRP, Gupta A, LeClair P (2020) Tuneable structure and magnetic properties in $Fe_{3-x}V_xGe$ alloys. J Alloys Compd 830:154403
11. Casper F, Felser C, Seshadri R, Sebastian CP, Pottgen R (2008) Searching for hexagonal analogues of the half-metallic half-Heusler XYZ compounds. J Phys Appl Phys 41(3):035002
12. Wang X, Cheng Z, Jin Y, Wu Y, Dai X, Liu G (2018) Magneto-electronic properties and tetragonal deformation of rare-earth-element-based quaternary heusler half-metals: a first-principles prediction. J Alloys Compd 734:329–341
13. Keshavarz S, Naghibolashrafi N, Jamer ME, Vinson K, Mazumdar D, Dennis CL, Ratcliff W, Borchers JA, Gupta A, LeClair P (2019) Fe_2MnGe: A hexagonal Heusler analogue. J Alloy Compd 771:793–802
14. Shanavas KV, McGuire MA, Parker DS (2015) Electronic and magnetic properties of Si substituted Fe_3Ge. J Appl Phys 118(12):123902
15. Drijver J, Sinnema S, Van der W F, (1976) Magnetic properties of hexagonal and cubic Fe_3Ge. J Phys F Met Phys 6(11):2165